JOURNAL OF GEOPHYSICAL RESEARCH, VOL. 104, NO. B2, PAGES 3013–3024, FEBRUARY 10, 1999

Influence of the shape of the friction law and fault finiteness on the duration of initiation

Ioan R. Ionescu[1]
Laboratoire de Mathématiques, Université de Savoie, Chambéry, France

Michel Campillo[2]
Laboratoire de Géophysique Interne, Observatoire de Grenoble, Université Joseph Fourier Grenoble, France

Abstract. We consider the two-dimensional (2-D) elastic problem of slip instability under slip dependent friction. This paper concentrates on the parameters that determine the duration of the initiation phase, that is, the delay between an initial small perturbation of the system at the metastable equilibrium and the onset of dynamic rupture propagation. We first consider the case of a homogeneous fault (i.e., with infinite length) with a slip dependent friction with varying weakening rate. We show that different laws associated with the same values of stress drop and critical slip lead to a broad range of initiation duration. The duration is mainly governed by the slope of the friction law at the origin. We interpret these results using the analytical solution proposed by *Campillo and Ionescu* [1997] for the case of a constant weakening rate. These late results suggest a definition of a characteristic length associated with the rate of weakening at the origin. When the region of slip is limited to a finite weak patch, we found that the duration of initiation varies rapidly when the fault length is of the order of the characteristic length. Under these conditions the initiation duration increases extremely rapidly with decreasing fault length up to about 100 s in the numerical experiments we carried out. These results suggest that very simple elastic models with slip dependent friction and realistic values of the parameters could explain a broad range of delay of the onset of rupture propagation.

1. Introduction

The finite duration of the initiation stage has been observed in laboratory experiments (see *Scholz* [1990] and *Ohnaka* [1996] for a review). *Iio* [1992, 1995] and *Ellsworth and Beroza* [1995] showed the signature of the initiation process in the onset at the very beginning of the seismograms. The problems of the evolution of the slip just prior to instability and of the delay between an initial perturbation and the onset of dynamic slip have been studied from the point of view of state dependant friction law [see *Dietrich*, 1994]. Our approach here is to consider only simple slip weakening laws and to study how this type of law can be associated with relatively large delays of onset. We study the duration of the initiation stage for the dynamic elastic problem of antiplane sliding under slip dependent friction. In a previous paper, *Campillo and Ionescu* [1997] presented an analytical solution for the problem of the growth of instability of slip on a fault with slip dependent friction. These results are limited to the case of a homogeneous fault with a simple friction law consisting of a weakening at constant rate until the critical slip is reached followed by a constant dynamic friction when the slip exceeds the critical slip (Figure 1, reference case). At the very beginning of the slip an analytic solution can be obtained quite easily since, in this case, the boundary condition on every point of the fault reduces to a linear boundary condition. This linearization is valid only in the initiation stage, that is, as long as the slip is less than the critical slip. From the analytical solution we reach the following conclusions concerning the delay of onset:

1. The delay has a weak logarithmic dependence on the initial perturbation.

2. The delay is inversely proportional to α_c, the ratio between the slope of the friction law and the shear modulus.

[1]Also at Laboratoire de Modélisation et Calcul, Institut d'Informatique et Mathématiques Appliquées, Grenoble, France

[2]Also at Institut Universitaire de France

Paper number 1998JB900090.
0148-0227/99/1998JB900090$09.00

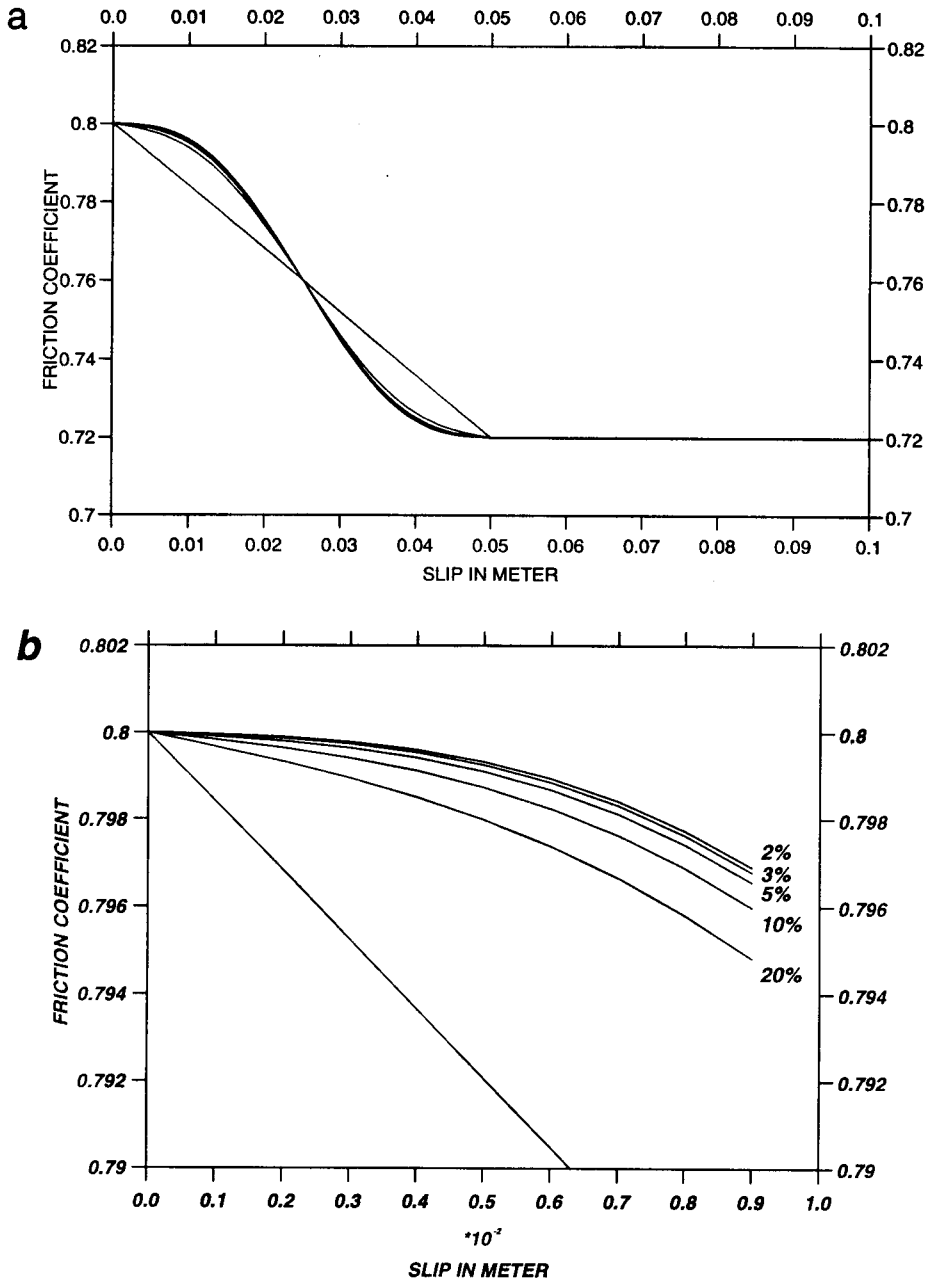

Figure 1. (a) Friction coefficient μ as a function of the relative slip δw. The reference friction law with linear weakening is plotted together with the five other laws investigated in this study. (b) Enlargement of the frictions laws in the vicinity of $\delta w = 0$.

When considering realistic values of the parameters of the friction laws, we expect the delay of onset to be very small, of order of 1 *s* [*Campillo and Ionescu*, 1997]. Our principal goal here is to explore how more complex configurations could lead to much larger times of onset as it is observed with the triggered seismicity or the occurrence of aftershocks, for example.

We consider here more complex friction laws for which the weakening rate changes with slip (see the recent experimental observations of *Ohnaka et al.* [1997]). In this case, when the instability develops, the weakening rate is different at the different points of the fault, and we obtain a heterogeous boundary condition on the fault. Hence we end with a heterogeneous problem even in the case of a fault with the same friction law everywhere. We use a numerical solution to study this problem, and we interpret the results in terms of the leading parameters deduced from the analytical treatment of the homogeneous problem. Finally, we consider the case when the slip can occur only on a patch with a finite length to study the influence of the length on the initiation time.

2. Problem Statement

Consider the antiplane shearing on a fault Γ_f in a homogeneous linear elastic space. Γ_f is in the plane $y = 0$. The contact on the fault is described by a slip dependent friction law. We assume that the displacement field is 0 in directions Ox and Oy and that u_z does not depend on z. The displacement is therefore denoted simply by $w(t,x,y)$. The elastic media have the shear rigidity G, the density ρ, and the shear velocity $c = \sqrt{G/\rho}$. The nonvanishing shear stress components are $\sigma_{zx} = \tau_x^\infty + G\partial_x w(t,x,y)$ and $\sigma_{zy} = \tau_y^\infty + G\partial_y w(t,x,y)$, and the normal stress on the fault plane is $\sigma_{yy} = -S$ ($S > 0$).

The equation of motion is

$$\frac{\partial^2 w}{\partial t^2}(t,x,y) = c^2\nabla^2 w(t,x,y) \tag{1}$$

for $t > 0$ and (x,y) not belonging to Γ_f. The boundary conditions on the fault Γ_f are

$$\sigma_{zy}(t,x,0+) = \sigma_{zy}(t,x,0-), \tag{2}$$

$$\sigma_{zy}(t,x,0) = \mu(\delta w(t,x))S\ \mathrm{sign}(\frac{\partial \delta w}{\partial t}(t,x)), \tag{3}$$

if $\partial_t \delta w(t,x) \neq 0$, and

$$|\sigma_{zy}(t,x,0)| \leq \mu(\delta w(t,x))S, \tag{4}$$

if $\partial_t \delta w(t,x) = 0$, where $\delta w(t,x) = w(t,x,0+) - w(t,x,0-$ is the relative slip and $\mu(\delta w)$ is the coefficient of friction on the fault.

The initial conditions are denoted by w_0 and w_1, that is,

$$w(0,x,y) = w_0(x,y), \quad \frac{\partial w}{\partial t}(0,x,y) = w_1(x,y). \tag{5}$$

3. Results of Linear Analysis

Since our intention is to study the evolution of the elastic system near an unstable equilibrium position, we shall suppose that $\tau_y^\infty = S\mu_s$, where $\mu_s = \mu(0)$ is the static value of the friction coefficient on the fault, which is supposed to be the plane $y = 0$. We remark that taking w as a constant satisfies (1)-(4); hence $w \equiv 0$ is a metastable equilibrium position, and w_0, w_1 may be considered as small perturbation of the equilibrium. For a small relative slip (i.e., if the perturbation is small enough) we may consider the linear approximation of the nonlinear function μ as follows:

$$\mu(\delta w) \approx \mu(0) + \mu'(0)\delta w. \tag{6}$$

We recall here some results of *Campillo and Ionescu* [1997] on the stability analysis in the special case of a linear friction law which is homogeneous on a fault with an infinite extension. The friction law has the form of a piecewise linear function:

$$\mu(\delta w) = \mu_s - \frac{\mu_s - \mu_d}{2L_c}\delta w \qquad \delta w \leq 2L_c, \tag{7}$$

$$\mu(\delta w) = \mu_d \qquad \delta w > 2L_c, \tag{8}$$

where μ_s and μ_d ($\mu_s > \mu_d$) are the static and dynamic friction coefficients and L_c is the critical slip. In this case the linear approximation (6) is valid for $\delta w \leq 2L_c$. For simplicity, let us assume in the following that the slip δw and the slip rate $\partial_t \delta w$ are nonnegative. Having in mind that we deal with a homogenous fault plane and with the evolution of one initial pulse, we may put (for symmetry reasons) $w(t,x,y) = -w(t,x,-y)$; hence we consider only one half-space $y > 0$ in (1) and (5). With these assumptions, (2)-(4) become

$$\frac{\partial w}{\partial y}(t,x,0+) = -\alpha_c w(t,x,0+) \qquad w(t,x,0+) \leq L_c, \tag{9}$$

$$\frac{\partial w}{\partial y}(t,x,0+) = -\alpha_c L_c \qquad w(t,x,0+) > L_c, \tag{10}$$

where α_c is a parameter which has the dimension of a wavenumber (m^{-1}) and which will play an important role in our further analysis. The value α_c is given by

$$\alpha_c = \frac{(\mu_s - \mu_d)S}{GL_c}. \tag{11}$$

It is important to note that α_c is proportional to the weakening rate. Since the initial perturbation (w_0, w_1) of the equilibrium ($w \equiv 0$) is small, we have $w(t,x,0+) \leq L_c$ for $t \in [0, T_c]$ for all x, where T_c is a critical time for which the slip on the fault reaches the critical value L_c at least at one point, that is, $\sup_{x\in R} w(T_c,x,0+) = L_c$. Hence for a first period $[0, T_c]$, called in the following initiation period, we deal with a linear initial and boundary value problem (equations (1), (5) and (9)).

Part of the solution has an exponential growth with time, while the other part has a wave type behavior, that is, without increase in amplitude. Hence, after a while the part with the exponential growth will completely dominate. This is why we put $w = w^d + w^w$, where w^d is the "dominant part" and w^w is the "wave part." Since the expression of the wave part w^w is not relevant for our analysis of the unstable growth, we give here only the simple expression of the dominant part:

$$w^d(t,x,y) = \frac{\alpha_c}{\pi}\exp(-\alpha_c y)\{\int_{-\alpha_c}^{\alpha_c}\int_0^\infty\int_{-\infty}^\infty$$

$$\exp(-\alpha_c s + i\alpha(x-u))[\cosh(ct\sqrt{\alpha_c^2-\alpha^2})w_0(u,s)$$

$$+\frac{\sinh(ct\sqrt{\alpha_c^2-\alpha^2})}{c\sqrt{\alpha_c^2-\alpha^2}}w_1(u,s)]dudsd\alpha\}. \tag{12}$$

This expression has the advantadge of allowing a direct simple computation of the solution at a given

time. It makes it possible to consider any type of initial perturbation not necessarily concentrated on the fault. The behavior of w can also be explained through a classical stability analysis of our initial and boundary value problem (see *Campillo and Ionescu* [1997]).

According to (12), the solution grows exponentially for wavenumber $|\alpha| < \alpha_c$. Therefore the characteristic half width of the slipping zone at the end of the initiation phase must be greater than a critical length l_c given by

$$l_c = \frac{\pi}{\alpha_c}. \tag{13}$$

This expression of the critical length, which has a form similar to the one proposed by *Dietrich* [1986, 1992] in a quite different context, is implied here by the unstable evolution of the system during the initiation phase.

Since the time evolution of the slip $w(t, x, 0+)$ is in essence described by the dominant part, we deduce that T_c satisfies $\sup_{x \in R} w^d(T_c, x, 0+) = L_c$. Assuming that the initial perturbation is such that the first point x of the fault for which the slip reaches the critical value L_c is $x = 0$, we obtain that T_c is the solution of the equation $w^d(T_c, 0, 0+) = L_c$.

Let us suppose that the initial perturbation is localized in an infinite strip $[-a, a] \times [b, +\infty[$ of half width a at the distance $b \geq 0$ from the fault $y = 0$; that is, $w_0(x, y) = w_1(x, y) = 0$ if $(x, y) \notin [-a, a] \times [b, +\infty[$. If b is different from zero, there is no perturbation of the slip (or slip rate) on the fault and only a perturbation of the displacement (or velocity) field in the bulk of the elastic body. This may correspond to the trigger of an earthquake by a distant source.

Let us introduce the following weighted average of the initial perturbation (as suggested by (12)):

$$W_0 = \frac{\alpha_c}{2a} \int_{-a}^{a} \int_{0}^{+\infty} \exp(-\alpha_c y) w_0(x, y) dx dy,$$

$$W_1 = \frac{\alpha_c}{2a} \int_{-a}^{a} \int_{0}^{+\infty} \exp(-\alpha_c y) w_1(x, y) dx dy.$$

If the initial perturbation is small and the half width is not too great, that is, $\pi L_c / [2a(W_0 \alpha_c + W_1/c)] \gg 1$ and $\pi/(a\alpha_c) \gg 1$, then from (12) one can deduce the following approximative formula given by *Campillo and Ionescu* [1997] :

$$T_c \approx \frac{b}{c} + \frac{1}{c\alpha_c} \ln\left[\frac{\pi L_c}{2a(W_0 \alpha_c + W_1/c)}\right]. \tag{14}$$

The term $T_w = b/c$ corresponds to the travel time needed by the waves associated with the initial perturbation to reach the fault. We remark that T_c depends on the initial average W_0 and W_1 through a natural logarithm, hence the duration of the initiation phase has only a weak (logarithmic) dependence on the amplitude of the initial perturbation.

The above formula is valid only for a linear dependence of the friction coefficient μ on the slip δw in the weakening domain ($\delta w \in [0, L_c]$, in our case). If a nonlinear weakening dependence $\mu = \mu(\delta w)$ is considered, a different evolution of the initiation phase can be expected (see section 5).

4. Numerical Approach

The theoretical development in section 3 indicates some strong and simple properties of the slip during the initiation phase. In particular, the essence of the evolution of the system is described by the exponential growth of the dominant part. The aim of this section is to propose a numerical scheme able to capture this instability for more complicated friction laws and for a nonhomogeneous fault.

Let us write the wave equation (1) as a first order hyperbolic system:

$$\rho \frac{\partial v}{\partial t}(t, x, y) = \frac{\partial \tau}{\partial y}(t, x, y) + \frac{\partial \sigma}{\partial x}(t, x, y) \tag{15}$$

$$\frac{\partial \tau}{\partial t}(t, x, y) = G \frac{\partial v}{\partial y}(t, x, y) \tag{16}$$

$$\frac{\partial \sigma}{\partial t}(t, x, y) = G \frac{\partial v}{\partial x}(t, x, y). \tag{17}$$

where $v(t, x, y) =: \partial_t w(t, x, y)$, $\tau(t, x, y) =: G \partial_y w(t, x, y)$, $\sigma(t, x, y) =: G \partial_x w(t, x, y)$.

Let Δt be the time step and let $\Delta x, \Delta y$ be the space steps such that $c\Delta t/\Delta x, c\Delta t/\Delta y \leq 1$. We shall consider two time-space grids (see Figure 2). The first one, $(n\Delta t, i\Delta x, (j - 1/2)\Delta y)$, will be used to solve the

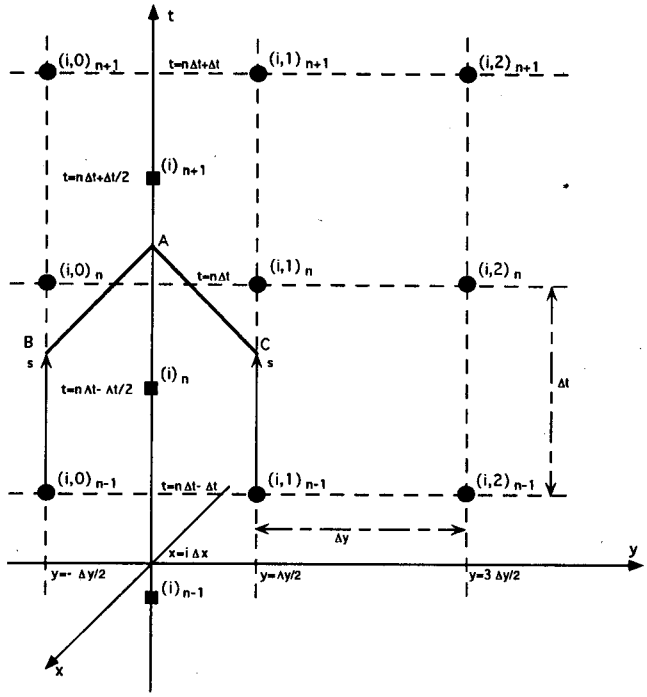

Figure 2. The interior time-space grid (solid circles) near the fault and the fault time-space grid (solid squares) at $x = i\Delta x$. AC and AB are the inward characteristic lines reaching the fault at time $t = (n-1/2)\Delta t + s$.

wave equation. We shall denote in the following by $v_{i,j}^n$, $\tau_{i,j}^n$, and $\sigma_{i,j}^n$ the discrete values of v, τ, and σ on this grid, that is $v_{i,j}^n = v(n\Delta t, i\Delta x, (j-1/2)\Delta y)$, $\tau_{i,j}^n = \tau(n\Delta t, i\Delta x, (j-1/2)\Delta y)$, and $\sigma_{i,j}^n = \sigma(n\Delta t, i\Delta x, (j-1/2)\Delta y)$.

The second grid, $((n+1/2)\Delta t, i\Delta x)$, is used to approach the friction law (3) on the fault $y = 0$. We shall denote by δw_i^n, δv_i^n, and $\bar{\tau}_i^n$, the values of δw, $\partial_t \delta w$, and τ on this grid, that is $\delta w_i^n = \delta w((n-1/2)\Delta t, i\Delta x)$, $\delta v_i^n = \partial_t \delta w((n-1/2)\Delta t, i\Delta x)$, and $\bar{\tau}_i^n = \tau((n-1/2)\Delta t, i\Delta x, 0)$.

Let us suppose that we know the solution on $(n\Delta t, i\Delta x, \pm 1/2\Delta y)$ and on $((n-1/2)\Delta t, i\Delta x)$ for some n. The numerical approach of the boundary condition (3) will give the solution (i.e., the relative slip and the stress) on $((n+1/2)\Delta t, i\Delta x)$ for $y = 0$. One can use now the stress distribution as a boundary condition at $y = 0$ for the wave equation and a classical finite difference method to deduce the solution on $((n+1)\Delta t, i\Delta x, (j-\frac{1}{2})\Delta y)$. Note that we need only the boundary conditions at $t \le (n+1/2)\Delta t$ to deduce the solution at $t = (n+1)\Delta t$ for $|y| \ge 1/2\Delta y$.

Since there are a lot of finite difference schemes to approach the wave equation, we will focus first on the boundary condition (3). To do this, let us think of (15) and (16) as a system in one space variable y for v and τ. Then after the integration on the characteristics lines (see Figure 2) we get

$$\frac{d}{ds}\delta w((n-\frac{1}{2})\Delta t+s,x)+\frac{2}{\sqrt{G\rho}}\tau((n-\frac{1}{2})\Delta t+s,x,0)=$$

$$v((n-1)\Delta t+s,x,c\frac{\Delta t}{2})-v((n-1)\Delta t+s,x,-c\frac{\Delta t}{2})+$$

$$\frac{1}{\sqrt{G\rho}}[\tau((n-1)\Delta t+s,x,c\frac{\Delta t}{2})+\tau((n-1)\Delta t+s,x,-c\frac{\Delta t}{2})]$$

$$+\frac{1}{\rho}\int_0^{\frac{\Delta t}{2}}[\frac{\partial\sigma}{\partial x}((n-1)\Delta t+s+\gamma,x,c(\frac{\Delta t}{2}-\gamma))$$

$$-\frac{\partial\sigma}{\partial x}((n-1)\Delta t+s+\gamma,x,-c(\frac{\Delta t}{2}-\gamma))]d\gamma, \quad (18)$$

for $s \in [0, \Delta t]$.

For the sake of simplicity, let us suppose that $\Delta x = \Delta y = c\Delta t$. Using a first order approximation of (18), we deduce

$$\frac{d}{ds}\delta w((n-\frac{1}{2})\Delta t+s,i\Delta x)+\frac{2}{\sqrt{G\rho}}\tau((n-\frac{1}{2})\Delta t+s,i\Delta x,0)$$

$$=A_i^n+\frac{s}{\Delta t}(B_i^n-A_i^n), \quad (19)$$

where

$$A_i^n=\delta v_i^n+\frac{2}{\sqrt{G\rho}}\bar{\tau}_i^n,\quad B_i^n=v_{i,1}^n-v_{i,0}^n+\frac{1}{\sqrt{G\rho}}(\tau_{i,1}^n+\tau_{i,0}^n)+$$

$$\frac{1}{4\sqrt{G\rho}}[(\sigma_{i+1,1}^n-\sigma_{i-1,1}^n)-(\sigma_{i+1,0}^n-\sigma_{i-1,0}^n)]+$$

$$\frac{1}{8}[(v_{i+1,1}^n+v_{i-1,1}^n-2v_{i,1}^n)-(v_{i+1,0}^n+v_{i-1,0}^n-2v_{i,0}^n)]-$$

$$\frac{1}{8\sqrt{G\rho}}[(\tau_{i+1,1}^n+\tau_{i-1,1}^n-2\tau_{i,1}^n)+(\tau_{i+1,0}^n+\tau_{i-1,0}^n-2\tau_{i,0}^n)].$$

If a slip event is present on the fault at $x = i\Delta x$ during the time interval $[(n-1/2)\Delta t, (n+1/2)\Delta t]$ then from (19) and the friction law we deduce the following nonlinear unstable differential equation:

$$\frac{d}{ds}\delta w((n-\frac{1}{2})\Delta t+s,i\Delta x)=-\frac{2S}{\sqrt{G\rho}}\mu(\delta w((n-\frac{1}{2})\Delta t+s,$$

$$i\Delta x))+A_i^n+\frac{s}{\Delta t}(B_i^n-A_i^n). \quad (20)$$

Let δt be the local time step, $N\delta t = \Delta t$ and let us denote $\delta w_i^{n,k} = \delta w((n-1/2)\Delta t+k\delta t, i\Delta x)$ with $\delta w_i^{n,0} = \delta w_i^n$. For $s \in [(k-1)\delta t, k\delta t]$ the nonlinear equation (20) can be approached by the linear differential equation:

$$\frac{d}{ds}\delta w((n-\frac{1}{2})\Delta t+s,i\Delta x)=c\alpha^{n,k}[\delta w((n-\frac{1}{2})\Delta t+s,i\Delta x)-$$

$$\delta w_i^{n,k-1}]+C_i^{n,k}+\frac{s-(k-1)\delta t}{\Delta t}(B_i^n-A_i^n)$$

where

$$\alpha^{n,k}=-\frac{2S}{G}\mu'(\delta w_i^{n,k-1}),$$

$$C_i^{n,k}=A_i^n-\frac{S}{\sqrt{G\rho}}\mu(\delta w_i^{n,k-1})+\frac{(k-1)\delta t}{\Delta t}(B_i^n-A_i^n).$$

The last linear equation can easily be solved to obtain

$$\delta w_i^{n,k}=\delta w_i^{n,k-1}+\frac{1}{c\alpha^{n,k}}\{[\exp(c\alpha^{n,k}\delta t)-1](C_i^{n,k}+$$

$$\frac{B_i^n-A_i^n}{\Delta t c\alpha^{n,k}})-\frac{(B_i^n-A_i^n)\delta t}{\Delta t}\}\ \text{if}\ \alpha^{n,k}\neq 0,$$

$$\delta w_i^{n,k}=\delta w_i^{n,k-1}+C_i^{n,k}\delta t+\frac{(B_i^n-A_i^n)(\delta t)^2}{2\Delta t}\ \text{if}\ \alpha^{n,k}=0.$$

From the numerical point of view, the method of integration of (20) is equivalent with the implicit Euler method and one iteration of the Newton method. However, the method presented above has the advantage of giving an exact integration of (20) in the case of a piecewise linear dependence of μ on the relative slip. Indeed, if the friction law is homogeneous on the fault plane, is a piecewise linear function given by (7), and $\delta w_i^{n,k-1} \le 2L_c$, then $\alpha^{n,k} = \alpha_c$, as expected from the theoretical stability analysis.

Finally, we put

$$\delta w_i^{n+1}=\delta w_i^{n,N},\quad \bar{\tau}_i^{n+1}=S\mu(\delta w_i^{n+1}),$$

$$\delta v_i^{n+1}=B_i^n-\frac{2}{\sqrt{G\rho}}\bar{\tau}_i^{n+1}.$$

If no slip event is present on the fault at $x = i\Delta x$ during the time interval $[(n-1/2)\Delta t, (n+1/2)\Delta t]$ then from (19) we get:

$$\delta w_i^{n+1}=\delta w_i^n,\quad \bar{\tau}_i^{n+1}=\frac{\sqrt{G\rho}}{2}B_i^n,\quad \delta v_i^{n+1}=0.$$

Concerning the discretization of the wave equation, we use an alternating direction method. The system (15)-(17) is reduced to two hyperbolic systems in one space dimension for each time step. The Lax-Wendroff (centered) finite differences scheme is used in the discretization of these systems. In order to compute the solution on the interior grid at time $t = (n+1)\Delta t$, we include the stress boundary condition $\bar{\tau}_i^{n+1}$ computed above from the friction law. Hence the process is iterated to the next time step.

In the case of a friction coefficient with a linear dependance with the slip, where the analytical solution can be obtained, the numerical results computed with this numerical approach were shown to be very accurate (see [*Campillo and Ionescu*, 1997].

5. Effect of the Shape of the Friction Law

We study the effect of the shape of the friction by considering several cases for which the friction static and dynamic coefficients and the critical slip are kept constant. As shown in Figure 1a, we consider a reference model with a constant weakening rate, and we add to it a sine-shaped modulation. While visually very similar, these different laws present significantly different slopes at the origin as it is shown in the enlargement in Figure 1b. The percentiles indicated in the Figure 1b give the ratio between the actual slope at the origin and the slope of the linear reference law. Indeed, our purpose is not to pretend that these particular functions are more relevant to the physics of earthquake than the more classical linear weakening. What we are tryning to demonstrate is the part played by the different characteristics of the laws to determine the timescale of the initiation process. Nevertheless, recent experimental results [*Ohnaka et al.*, 1997] show that the type of slip dependence used here is close to the observations. The shape of the weakening is discussed in terms of fault surface properties by *Matsu'ura et al.* [1992] and from the point of view of micromechanics by *Yoshioka* [1997].

We use a grid of 800 × 800 points in the x, y plane. We consider the following model parameters: $\rho = 3000$ kg/m^3, $c = 3000$ m/s, $L_c = 0.05$ m, $\mu_s = 0.8$, and $\mu_d = 0.72$. The normal stress is assumed to correspond to a lithostatic pressure at a depth of 5 km. Considering an infinite homogeneous fault, we compute the development of the instability after an initial perturbation given by

$$w_1(x,y) = v_0 \exp\left(\frac{(x-x_0)^2}{(x-x_0)^2 - a^2}\right) \quad |x-x_0| < a \quad |y| < b,$$
$$w_1(x,y) = 0 \quad \text{elsewhere}, \tag{21}$$

where the half width a is 4000 m, the maximum amplitude v_0 is 0.00001 m/s, and b is equal to 250 m.

In order to perform the computations for long time windows, we have to use a relatively coarse discretization in space and time. We have to check that in the range used here, the grid spacing does not affect the results. We perform a series of computations in exactly the same conditions, except for the grid spacing. We consider values of Δx of 31.25, 125, and 500 m. We present in Figure 3 a comparison of the slip velocities computed at the point of the fault at the center of the zone where the initial perturbation is applied. The friction law has a slope at the origin of 20% of the slope of the linear case (Figure 1). Since $\Delta t = \Delta x/c$, one can easily recognize the curve corresponding to the larger grid point appearing as a piecewise linear curve. This

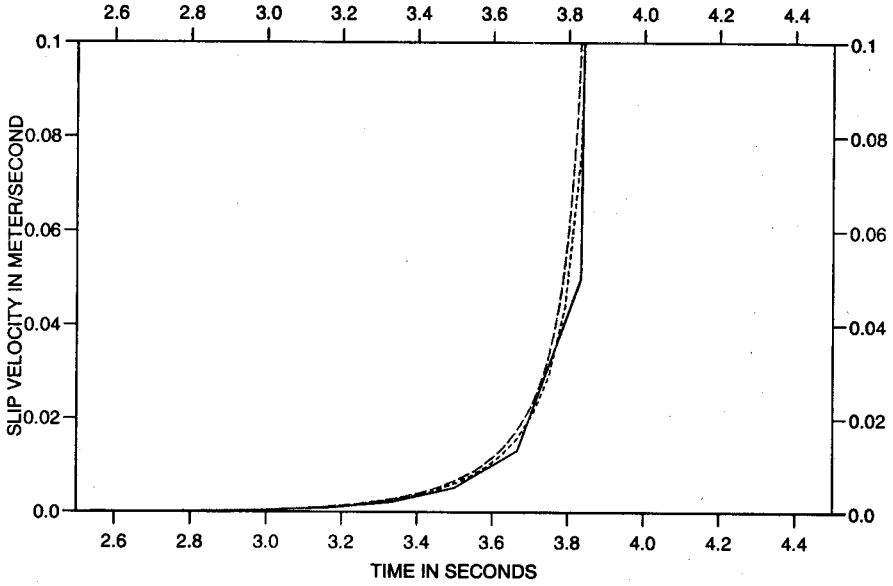

Figure 3. Comparison of slip velocity ($\partial_t \delta w(t,0)$) computed at the center of the zone where the initial perturbation is applied with grid spacings Δx of 31.25 m (long-dashed line), 125 m (short-dashed line), and 500 m (solid line) and $\Delta t = \Delta x/c$.

comparison shows that even with very coarse discretization, the numerical scheme is accurate enough to simulate the initiation phase. The delay of onset obtained is the same for the three discretizations. This test shows the possibility of using coarse grids to investigate relatively long delay of onset. In all the computations presented here, we checked that the initiation develops as a smooth exponential-like growth in order to identify numerical noise. Since the initial growth can be very slow, it can occur that the numerical noise due to computer roundup dominates over the expected evolution process. As it will be discussed later, it is a limitation of the study of slow initiation process by numerical methods.

To illustrate the computations done here, we present in Figure 4 two examples of computations done for the case of a linear weakening (Figure 4a) and the case of a slope at the origin of 20% of the slope of the linear case (Figure 4b). Figures 4a and 4b show the slip velocity on the fault as a function of position and time. The perturbation (21) is applied at time $t = 0$. In the case of the linear weakening, the rupture front begins to propagate about 1 s after the perturbation. The rupture thus develops as a crack with a slip velocity concentration that propagates at the shear wave velocity. In the case of the nonlinear friction law the rupture front appears with a delay of about 4 s after the perturbation is applied. This example illustrates the importance of the slope at the origin of the friction law for the delay of the onset of the dynamic instability. One can also notice in Figure 4 the difference in the amplitude of the slip velocity concentration. It has a weaker amplitude in the case of the nonlinear law. As for the delay of onset, this difference of amplitude is also due to the shape of the friction law, but in this last case the critical feature is the shape of the friction law at the end of the weakening. Effectively, for a propagative rupture front, the slip velocity at a point increases exponentially in the weakening stage, then decreases sharply when the friction becomes constant, that is, when the slip reaches its critical value $2L_c$. As it is shown in Figure 1, for the nonlinear friction law the end of the weakening phase is characterized by a smooth evolution toward the constant friction, while in the linear case the friction law exhibits a kink at $\delta w = 2L_c$, that is, 0.05 m in our case. The difference in slip velocity amplitude shown in Figure 3 reflects the difference in the transition between weakening and dynamic constant friction for the two friction models. The piecewise linear friction law is associated with higher peak slip velocity because the transition between weakening and constant dynamic friction is sharper in this case.

We perform a series of tests for the different friction laws depicted in Figure 1. The computations are done from the initial time of perturbation up to the time when the rupture begins to propagate. We present in Figure 5 the slip velocity obtained for the friction laws shown in Figure 1. Again, the time series correspond to

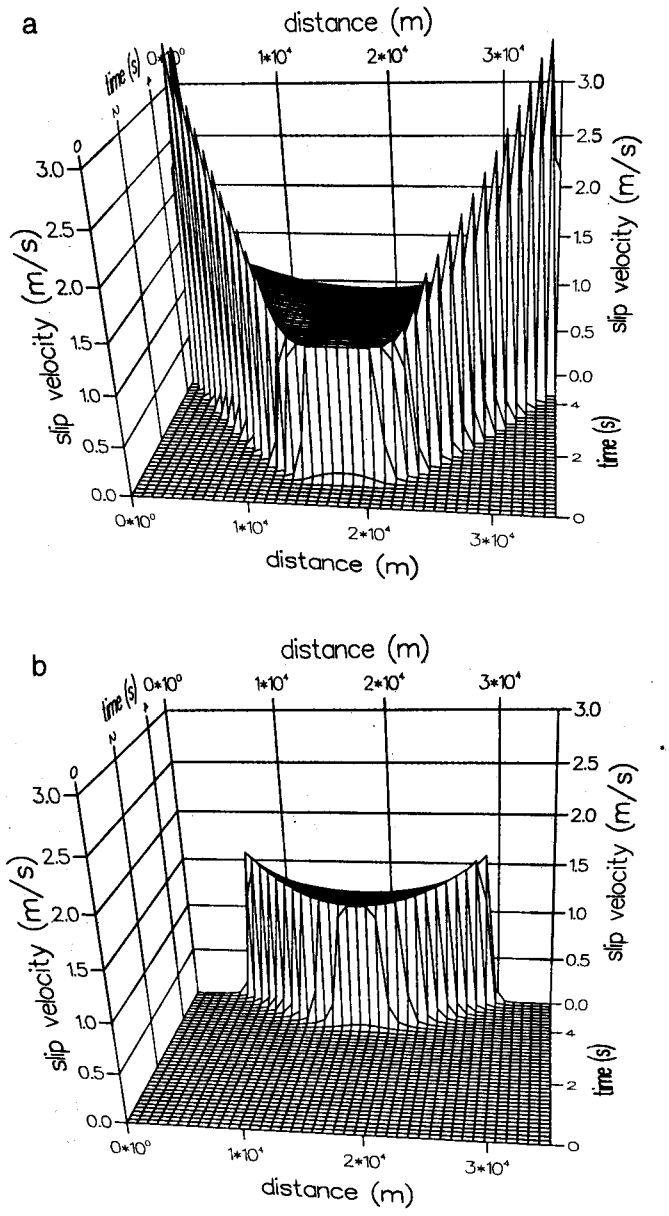

Figure 4. (a) Slip velocity ($\partial_t \delta w(t, x)$) on the frictional surface ($y = 0$) as a function of space x and time t for the linear reference friction law. (b) Slip velocity ($\partial_t \delta w(t, x)$) in the case of a nonlinear weakening with a slope at the origin of 20% of the slope of the linear case as shown in Figure 1.

the point of the fault at the center of the zone where the initial perturbation is applied. The initial perturbation has the same amplitude in all the cases. The reference case with a linear weakening corresponds to the curve without a label. The other time series are displayed with a label giving the slope characteristics of the different friction laws. We present the slip velocity in the range 0-0.1 m/s since it is sufficient to visualize the steep increase of slip velocity corresponding to the onset of the propagating rupture front as shown in Figure 4. Figure 5 indicates that with the same static and dynamic coefficients and the same critical slip, the time of

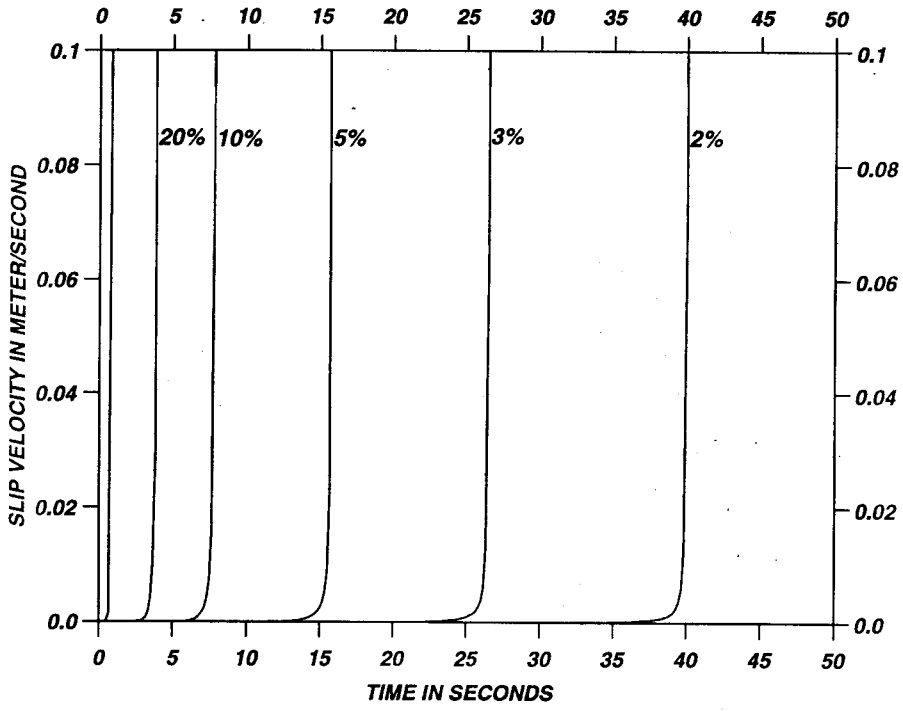

Figure 5. Slip velocities ($\partial_t \delta w(t,0)$) at the center of the zone where the initial perturbation is applied for the six friction laws depicted in Figure 1. All other parameters were kept identical. The labels indicate the rate of weakening at the origin with respect to the case of the linear weakening. The linear case has no label and corresponds to the shortest delay.

onset can be very different. While the onset of rupture propagation occurs in 1 s after the initial perturbation in the reference linear law, the initiation phase lasts for 40 s in the case of the law with initial slope of 2% of the reference one.

We learned from the analytical solution of the homogeneous problem that the evolution of the slip in the initiation phase is conditionned by the rate of weakening. In the example of the nonlinear friction law presented here, one can expect the initial slope to play a prominant part for the duration of the initiation phase. Actually, since the slope is very small at the origin, the growth will be very slow at the beginning of the initiation. This early stage dominates the duration since we expect the rate of growth to be exponential but with a small exponent when the slope of the friction law at the origin is small (see equation (12)). Although this analysis is rather crude, the numerical results show that it can be useful for a first-order interpretation. According to the theory of the homogeneous case, we expect the delay of onset to vary almost linearly with the inverse of the slope of the friction law at the origin (see equation (14)). We present in Figure 6 the delay of onset measured on the curves of Figure 5 as a function of the inverse of the initial slope of the corresponding friction law. The dependance is almost perfectly linear in the range of values considered here. This result led us to the following extrapolation of the theoretical results of the homogeneous problem to the complex case of a nonlinear friction law. Indeed, using the linear approximation (6), we can define

$$\alpha_c = -\frac{2S}{G}\mu'(0). \tag{22}$$

So, α_c has same the physical meaning as in the case of the constant weakening rate. Moreover, as it was shown from the numerical tests, the expression (14) for T_c is still valid with α_c given by (22).

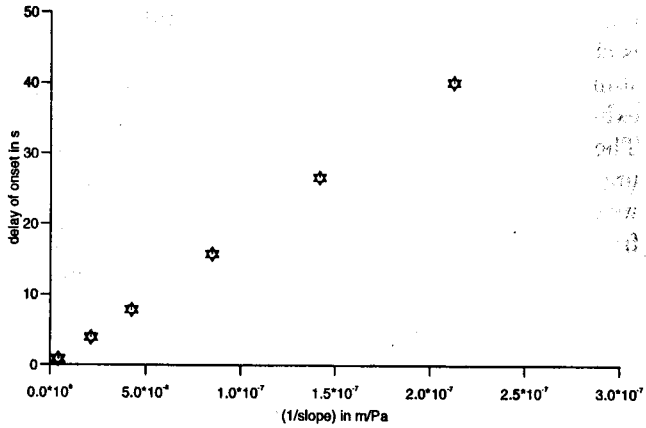

Figure 6. Delay of onset measured on the curves of Figure 5 as a function of the inverse of the slope of the friction law at the origin (i.e. $1/(2S\mu'(0))$). Note the linear dependence.

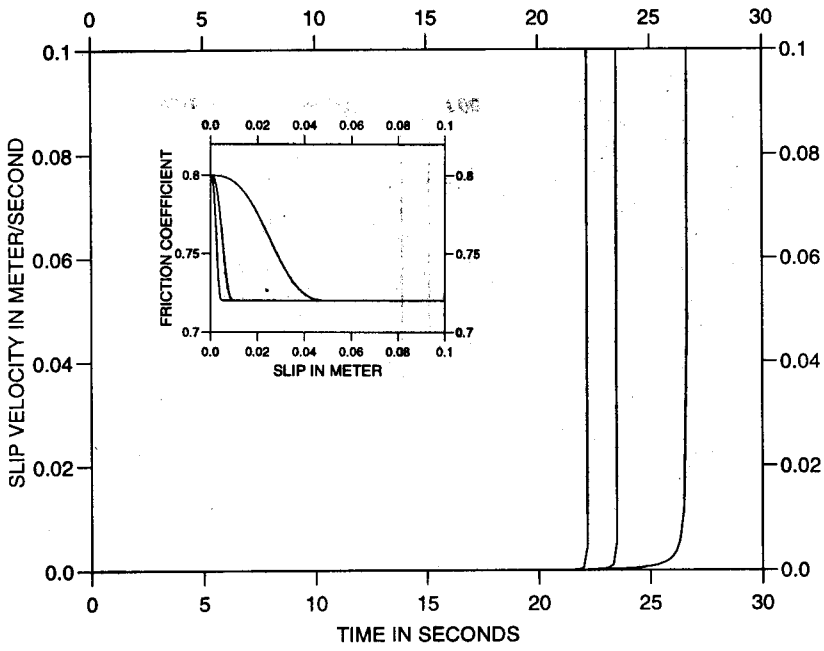

Figure 7. Slip velocities ($\partial_t \delta w(t,0)$) at the center of the zone where the initial perturbation is applied for three friction laws presented in the box. The friction laws have different critical slip but have the same rate of weakening at the origin.

Unfortunately we are not able to extend our numerical tests toward larger delays because of the limitation of computer accuracy. To verify that the initial slope is effectively the relevant parameter, we performed numerical tests in which we kept constant the initial slope of the law while changing the value of L_c. We present in Figure 7 such a test in which a computation is repeated for three friction laws corresponding to different values of L_c while all the parameters not related to the friction law are identical. The friction laws have the same initial rate of weakening and critical slip of 0.005, 0.01 and 0.05 m. In spite of a change of L_c of one order of magnitude, the delay varies only 18% in this example. As expected, the delay of onset is only weakly dependant on the absolute value of L_c.

The conclusion drawn from the computations shown in this section is that the delay of onset is strongly dependent on the detail of the friction law in the neighborhood of the origin. In contrast the parameters often used to characterize the friction law, that is, the friction drop and the critical slip, are not sufficient to infer, even grossly, the delay of onset.

6. Effect of the Finite Length of the Fault

Let us consider now the case of a finite fault of length l_f. We define the fault as the weak patch when the slip can develop. On the rest of the surface $y = 0$, the static friction is so large that it cannot be reached. In conclusion, we add to (1) and (5) the following boundary conditions: (2)-(4) are satisfied for $|x| < 1/2 l_f$,

$$\delta w(t,x) = 0 \quad \text{for} \quad |x| > \frac{1}{2} l_f. \tag{23}$$

We set the friction law of the fault equal to the one used in the previous section 5 with a slope at the origin of 3% of the slope of the linear law (see Figure 1). The stress before the application of a perturbation is equal to the static friction. To illustrate the effect of fault finiteness, we present in Figure 8 a computation in which the fault

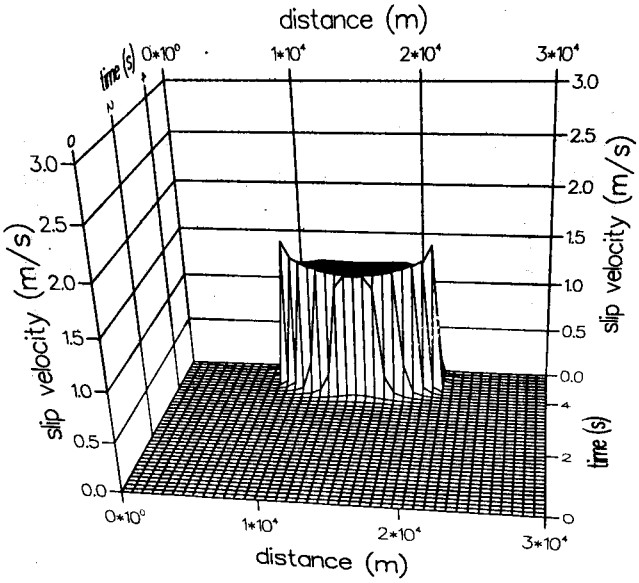

Figure 8. Slip velocity ($\partial_t \delta w(t,x)$) on the frictional surface ($y = 0$) as a function of space x and time t computed in the same conditions as in Figure 4b except for the fact that the fault is now of finite length $l_f = 15,000$ m.

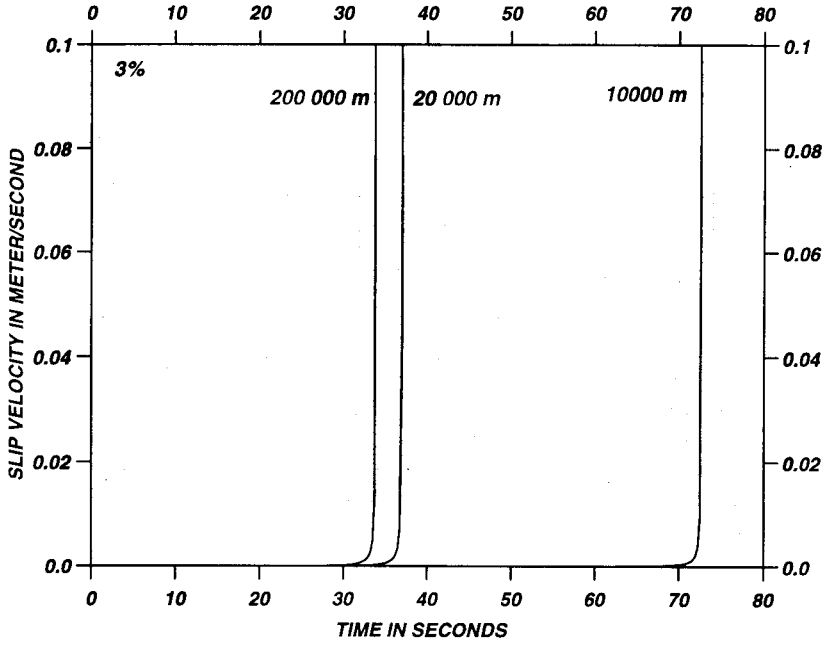

Figure 9. Slip velocities ($\partial_t \delta w(t,0)$) at the point which is in the same time center of the zone where the initial perturbation is applied and the center of the finite fault. The fault lengths l_f considered are 200,000, 20,000 and 10,000 m. The rate of weakening at the origin is 3% of the reference linear one, corresponding to a characteristic length of $l_c = 11,900$ m.

has an extent l_f of 15,000 m while all parameters are kept similar to the computation shown in Figure 4b. In this particular case, the fault finiteness does not affect the development of the initiation, and the time of the beginning of the rupture is the same for the finite and the infinite fault. Indeed, this is not a general feature, as it will be shown with the next set of computations. We consider a series of faults of different lengths. The initial perturbation has the same form as in the previous examples except for a, the half width of the zone where the perturbation is applied, which is now 2000 m. We consider the friction law with a slope at the origin of 3% of the linear reference slope. We present in Figure 9 the slip velocities obtained at a point on the fault at the center of the zone where the initial perturbation is applied, which is also the center of the weak zone. The computations are done from the initial time up to the point when the rupture propagates. We consider 3 different fault lengths: $l_f = 200,000, 20,000$ and 10,000 m. The delay of onset increases for decreasing fault length in a very nonlinear way. Changing the fault length from 200,000 m to 20,000 m adds only a few seconds to a delay which is about 34 s for an infinite fault. On the other hand, when the fault length is changed from 20,000 m to 10,000 m, the delay changes from 37 to 73 s.

To understand why this drastic change occurs in this fault length range, we propose to scale the problem with respect to the properties of the friction law. We showed in section 5 that in the case of an infinite fault and of a complex friction law the initiation process is well understood through a generalization of the analytical results obtained for a linear friction law. We concluded that at the first order, the leading parameter is the weakening rate at the origin. We can further use this approach by defining the characteristic half length l_c associated with the friction law according to (13) and (22):

$$l_c = -\frac{\pi G}{2S\mu'(0)}. \tag{24}$$

In the present computation the characteristic half length l_c defined for an infinite fault (equation (24)) and associated with the slope at the origin is 11,900 m. The numerical results of Figure 7 indicate that the variation of delay with fault length seems much faster when the fault length is of the order of the characteristic length associated with the friction. It is very difficult to investigate with finite difference simulations delay times which are much larger than the 73 s obtained here. Nevertheless, this amazingly long delay suggests that a sharp transition of behavior occurs when the fault length is of the order of the characteristic length associated with the slope of the friction law at the origin.

We performed a series of numerical tests in which we systematically changed the fault length and the amplitude of the initial perturbation to study the form of the dependance of the duration of initiation on these parameters. For practical reasons, we performed these computations with the friction law with an initial slope of 5% of the reference one (Figure 1) for which the characteristic length l_c defined for an infinite fault (equation (24) is 7200 m. To summarize the results, we plotted

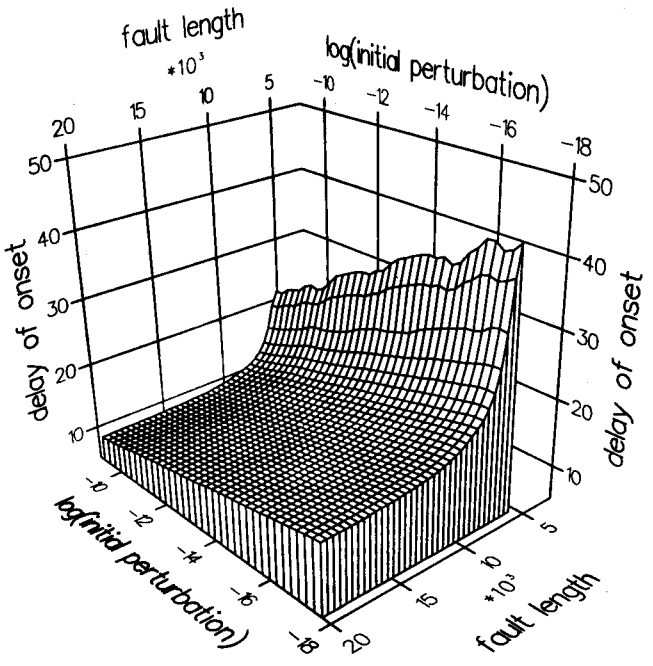

Figure 10. Delay of onset as a function of the fault length l_f and of the logarithm of the amplitude of the initial perturbation v_0. It was not possible to perform the computation for smaller fault lengths, as stated in the text.

the delay as a function of the amplitude of the initial perturbation and of the fault length. The amplitude of the initial perturbation is proportional to the parameter v_0 of (21). The results are presented in Figure 10. The small fluctuations visible for the largest values of delay are due to the interpolation of the 50 values effectively computed. These results show that the delay of onset varies linearly with the logarithm of the amplitude as expected from the theory of the homogeneous problem (equation (14)). On the other hand, the behavior of the delay with the length of the fault is much more complex. Clearly, when the fault length is larger than the characteristic length of the friction (i.e., $l_f >> l_c$), the delay of onset is almost independent of the fault length, governed only by the characteristics of the friction law. When the fault length approaches the characteristic half length (i.e., $l_f \approx l_c$), the delay increases extremely rapidly. Unfortunately, we are not able to compute the cases where the delay is very large. In these conditions, for decreasing l_f values it is not clear if the delay is increasing to large finite values or if the instability is unable to develop. Both possibilities are considered to be acceptable after our numerical tests while their implications could be drastically different. This point may be clarified from the point of view of elastostatics. The fault length for which the transition between stable sliding and stick slip occurs can be approximatively estimated by a static stability analysis. The simplest one uses an analogy with a block slider system. In this case, one expects that the transition occurs when the stiffness of the system is equal to the weakening rate. According to a static analysis of a crack, the "stiffness" of the fault is of the order G/l_f . This indicates that the limit of stability is when l_f is of the order of l_c given by (24). This simple argument shows that there exists a lower limit of the fault length for which an instability can develop. Nevertheless, we remark that l_c defined as for the infinite fault problem (equation (24)), which is 7200 m here, does not represent strictly the minimum size of the sliding patch, which is about 5400 m. In order to obtain a more precise evaluation of the critical fault length a more complicated stability analysis has to be considered (see *Ionescu and Paumier* [1996] for some general results in the case of a finite domain). A complete mathematical treatement, which gives the expression of the critical length of the fault patch, requires complex analytical and numerical developments which are still in progress.

The dynamic process can be characterized by the coefficient of a time exponential as suggested by (12). For $l_f >> l_c$ this coefficient is independant of l_f. When l_f is of the order of l_c, our results suggest that it decreases with l_f up to a point where l_f reaches a critical value for which the system enters a stable sliding regime for which this coefficient tends to 0 and therefore T_c tends to infinity. Our results indicate that large delays of rupture can be expected for elastic systems with simple friction laws.

The fact that the delays of rupture are large, has straightforward implications for the evolution on a complex fault. After the rupture of an elementary patch, a neighbor fault patch close to the failure could sustain the corresponding perturbation for quite a long time. The delay can be sufficiently long to make the induced rupture apparently uncorrelated with the initial event. The same type of arguments can be invoked for the delay between a main event and its aftershocks. We found a strong sensitivity of the delay to both the details of the friction law and the length of the weak patch able to slip. This can explain the wide range of delay between the main shock and the aftershocks that occur on various fault segments with different length and probably different friction properties.

7. Conclusion

We present a numerical study of the 2-D elastic problem of slip instability under slip dependent friction. We concentrate our analysis on the parameters that determine the duration of the initiation phase, that is, the delay between an initial small perturbation of the system at the metastable equilibrium and the onset of dynamic rupture propagation. We first consider the case of a homogeneous fault (i.e., with infinite length) with a slip dependent friction with varying weakening rate. Our results show that different laws associated with the same values of stress drop and critical slip lead to a broad range of initiation duration. The duration is

governed mainly by the slope of the friction law at the origin. These results can be interpreted qualitatively using the analytical solution proposed by *Campillo and Ionescu* [1997] for the case of a constant weakening rate. These late results suggested a definition of a characteristic length associated with the rate of weakening at the origin. When considering a fault of finite length, we found that the duration of initiation varies rapidly when the fault length is of the order of the characteristic length. Under these conditions the initiation duration increases extremely rapidly with decreasing fault length up to 100 s in the numerical experiments we carried out. These results suggest that very simple elastic models with slip dependent friction and realistic values of the parameters could explain a broad range of delay of the onset of rupture propagation after a perturbation. This could contribute to the apparent temporal decorrelation between earthquakes and the causes of perturbation of the mechanical conditions on the fault (such as distant earthquakes or tides).

Acknowledgments. We acknowledge financial support from Institut de Protection et de Sureté Nucléaire and from project SIGMAS of IMAG (Université Joseph Fourier). Numerical simulations were performed at the Centre de Calcul Intensif de l'Observatoire de Grenoble. We thank G. Beroza, M. Ohnaka, and an anonymous reviewer for their comments and their suggestions to improve this paper.

References

Campillo, M., and I.R. Ionescu, Initiation of antiplane shear instability under slip dependent friction, *J. Geophys. Res., 102*, 20,263-20,371, 1997.

Dietrich, J.H., A model for the nucleation of earthquake slip, in *Earthquake source mechanics, Geophys. Monogr. Ser.*, vol. 37, edited by S. Das, J. Boatwright, and C.H. Sholz, pp. 37-47, AGU, Washinton, D. C., 1986.

Dietrich, J.H., Earthquake nucleation on faults with rate- and state-dependent strength, *Tectonophysics, 211*, 115-134, 1992.

Dietrich, J.H., A constitutive law for rate of earthquake production and its application to earthquake clustering, *J. Geophys. Res., 99*, 2601-2618, 1994.

Ellsworth, W.L., and G.C. Beroza, Seismic evidence for an earthquake nucleation phase, *Science, 268*, 851-855, 1995.

Iio, Y., Slow initial phase of the P-wave velocity pulse generated by microearthquakes, *Geophys. Res. Lett., 19(5)*, 477-480, 1992.

Iio, Y., Observations of the slow initial phase generated by microearthquakes: Implications for earthquake nucleation and propagation, *J. Geophys. Res.*, 100, 15333-15349, 1995.

Ionescu, I.R., and J.-C. Paumier, On the contact problem with slip dependent friction in elastostatics, *Int. J. Eng. Sci., 34*(4), 471-491, 1996.

Matsu'ura, M., H. Kataoka, and B. Shibazaki, Slip dependent friction law and nucleation processes in earthquake rupture, *Tectonophysics, 211*, 135-148, 1992

Ohnaka, M., Nonuniformity of the constitutive law parameters for shear rupture and quasistatic nucleation to dynamic rupture: A physical model of earthquake generation model, paper presented at Earthquake Prediction: The Scientific Challenge, U.S. Acad. of Sci., Irvine, Calif., 1996.

Ohnaka, M., M. Akatsu, H. Mochizuki, A. Odedra, F. Tagashira, and Y. Yamamoto, A constitutive law for the shear failure of rock under lithospheric conditions, *Tectonophysics, 277*, 1-28, 1997.

Scholz, C.H., The Mechanics of Earthquakes and Faulting, Cambridge Univ. Press, New York, 1990.

Yoshioka, N., A review of the micromechanical approach to the physics of contacting surfaces, *Tectonophysics, 277*, 29-40, 1997.

I. R. Ionescu, Laboratoire de Mathématiques, Université de Savoie, 73376 Le Bourget-du-Lac Cedex, France. (e-mail: Ioan.Ionescu@univ-savoie.fr)

M. Campillo, Laboratoire de Géophysique Interne, Observatoire de Grenoble, Université Joseph Fourier, BP 53X, 38041 Grenoble Cedex, France (e-mail: Michel.Campillo@obs.ujf-grenoble)

(Received February 4, 1998; revised September 18, 1998; accepted November 11, 1998.)